12-1-2015

Unveiling the Crucial Intermediates in Androgen Production

Piotr J. Mak
Marquette University, piotr.mak@marquette.edu

Michael C. Gregory
University of Illinois at Urbana-Champaign

Ilia G. Denisov
University of Illinois at Urbana-Champaign

Stephen G. Sligar
University of Illinois at Urbana-Champaign

James R. Kincaid
Marquette University, james.kincaid@marquette.edu

Accepted version. Proceedings of the National Academy of Sciences, Vol 112, No. 52 (December 2015): 15856-15861. DOI.

Unveiling the Crucial Intermediates in Androgen Production

Piotr J. Mak
Department of Chemistry, Marquette University, Milwaukee, WI
Michael C. Gregory
Department of Biochemistry, University of Illinois, Urbana, IL
Ilia G. Denisov
Department of Biochemistry, University of Illinois, Urbana, IL
Stephen G. Sligar
Department of Biochemistry, Department of Chemistry, College of Medicine, University of Illinois, Urbana, IL
James R. Kincaid
Department of Chemistry, Marquette University, Milwaukee, WI,

Proceedings of the National Academy of Sciences, Vol 112, No. 52 (December 2015): pg. 15856-15861. DOI.

Significance: The human enzyme cytochrome P450 17A1 (CYP17A1) catalyzes the critical step in the biosynthesis of the male sex hormones, and, as such, it is a key target for the inhibition of testosterone production that is necessary for the progression of certain cancers. CYP17A1 catalyzes two distinct types of chemical transformations. The first is the hydroxylation of the steroid precursors pregnenolone and progesterone. The second is a different reaction involving carbon–carbon (C-C) bond cleavage, the mechanism of which has been actively debated in the literature. Using a combination of chemical and biophysical methods, we have been able to trap and characterize the active intermediate in this C-C lyase reaction, an important step in the potential design of mechanism-based inhibitors for the treatment of prostate cancers.

Keywords: cytochrome P450, steroids, nanodiscs, peroxo-hemiacetal, resonance Raman spectroscopy

Abstract: Ablation of androgen production through surgery is one strategy against prostate cancer, with the current focus placed on pharmaceutical intervention to restrict androgen synthesis selectively, an endeavor that could benefit from the enhanced understanding of enzymatic mechanisms that derives from characterization of key reaction intermediates. The multifunctional cytochrome P450 17A1 (CYP17A1) first catalyzes the typical hydroxylation of its primary substrate, pregnenolone (PREG) and then also orchestrates a remarkable C_{17}–C_{20} bond cleavage (lyase) reaction, converting the 17-hydroxypregnenolone initial product to dehydroepiandrosterone, a process representing the first committed step in the biosynthesis of androgens. Now, we report the capture and structural characterization of intermediates produced during this lyase step: an initial peroxo-anion intermediate, poised for nucleophilic attack on the C_{20} position by a substrate-associated H-bond, and the crucial ferric peroxo-hemiacetal intermediate that precedes carbon–carbon (C-C) bond cleavage. These studies provide a rare glimpse at the actual structural determinants of a chemical transformation that carries profound physiological consequences.

The excessive production of androgen, which effectively fuels the progression of cancer, especially prostate cancer, was first treated by surgical methods,[1] whereas more modern approaches are focused on the discovery and development of pharmaceuticals that can selectively inhibit androgen synthesis.[2,3] A member of the cytochrome P450 superfamily,[4,5] cytochrome P450 17A1 (CYP17A1), occupies a central role in the biosynthesis of steroid hormones in humans. As was first reported by Nakajin and Hall[6] and Nakajin et al.[7] for CYP17 from pig testis, this enzyme catalyzes two fundamentally different types of chemical transformations,[5-11] with the first being the efficient hydroxylation of both of its primary substrates, pregnenolone (PREG) and progesterone (PROG), to 17-hydroxypregnenolone (17-OH) PREG

Proceedings of the National Academy of Sciences, Vol 112, No. 52 (December 2015): pg. 15856-15861. DOI.

and 17-hydroxypregnenolone, respectively (Fig. 1). Importantly, 17-OH PREG is further processed in a second step in which CYP17A1 now catalyzes, not another hydroxylation reaction, but a complex 17,20 carbon–carbon (C-C) bond cleavage (lyase) reaction. This step converts 17-OH PREG to dehydroepiandrosterone (DHEA), a process that represents a critical branch point in human steroidogenesis by providing the essential precursor to androgens and various corticosteroids.[5-9] Although a similar C-C bond cleavage of 17-OH PROG is also mediated by CYP17A1, it is of less importance in humans because its efficiency is only about 2% of the efficiency of the physiologically important lyase reaction involving 17-OH PREG.[10] Recognizing the intensive efforts currently underway to design and test substances that selectively inhibit CYP17A1,[2,3] there is a pressing need to enhance our understanding of the relevant reaction mechanisms, a task that typically entails identification of key reaction intermediates. Directly addressing this issue, we report the successful capture and structural characterization of these elusive species, providing convincing evidence that in the presence of PREG, the enzyme active site is organized to facilitate the hydroxylation reaction, whereas the 17-hydroxyl group of the 17-OH PREG substrate directly interacts with the ferric peroxo-intermediate to promote the C-C bond cleavage process effectively.

Proceedings of the National Academy of Sciences, Vol 112, No. 52 (December 2015): pg. 15856-15861. DOI.

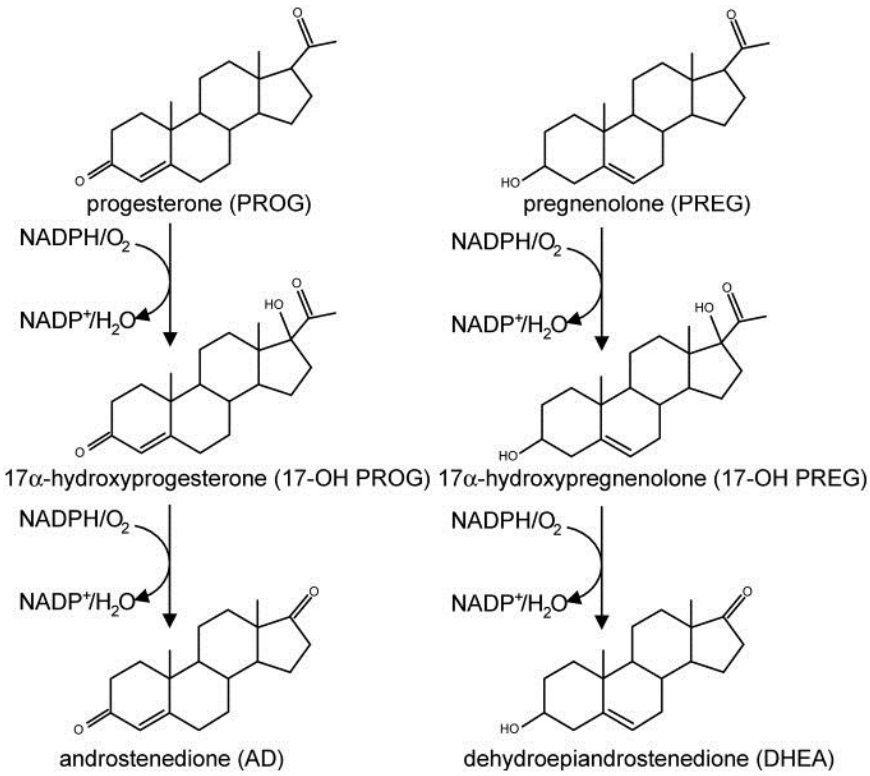

Fig. 1. Proposed pathway for biosynthesis of androstenedione and DHEA catalyzed by human CYP17A1.[4,5]

As depicted in the enzymatic cycle illustrated in Fig. 2,[4,5] binding of substrate induces a low-spin (LS) to high-spin state conversion of the heme prosthetic group, whose attendant change in reduction potential triggers electron transfer from an associated reductase, with the resulting ferrous protein readily binding molecular oxygen to form a semistable dioxygen adduct, properly viewed as a ferric-superoxide species. This complex is the last intermediate in the cycle that can be conveniently studied by conventional spectroscopic methods. Delivery of a second electron produces a reactive ferric peroxo-intermediate.[4,5] In the vast majority of cases, as depicted by the green arrows appearing in the circular reaction cycle illustrated in Fig. 2, this peroxo-intermediate accepts the rapid sequential delivery of two protons. The first forms a fleeting hydroperoxo-intermediate, which rapidly undergoes O-O bond cleavage upon delivery of the second proton to generate a highly reactive "compound I" species, whose impressive ability to effect hydroxylation and certain other difficult chemical transformations is widely appreciated.[4,5] Recent efforts by

Proceedings of the National Academy of Sciences, Vol 112, No. 52 (December 2015): pg. 15856-15861. DOI.

Green and coworkers[12,13] have provided further definition of the structure and reactivity of compound I.

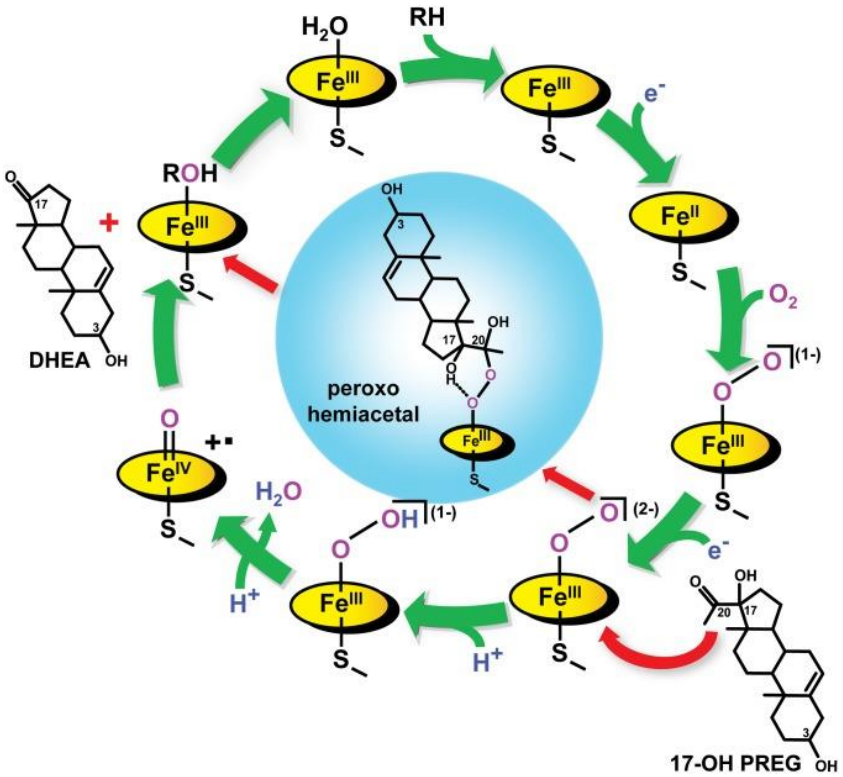

Fig. 2. Cytochrome P450 enzymatic cycle and formation of a peroxo-hemiacetal intermediate.

There are critical physiological demands for other types of difficult substrate transformations that are not effectively mediated by compound I. A prime example is encountered in vertebrates, where at least 14 CYPs are involved in the transformation of cholesterol into a relatively large number of physiologically required steroid hormones, including androgens, estrogens, and corticosteroids.[4,14] Although the classical hydroxylation reactions are most frequently encountered in these schemes, a few of these important CYPs are multifunctional, orchestrating complex sequential reactions that result in unusual C-C bond cleavage processes. Although such dramatic chemical transformations are well documented, much uncertainty remains about how these multistage reaction sequences actually proceed.[5,9]

Our present work focuses on the membrane-bound CYP17A1, whose chimeric reactivity patterns are controlled, in large part, by the

Proceedings of the National Academy of Sciences, Vol 112, No. 52 (December 2015): pg. 15856-15861. DOI.

precise molecular structure of the particular substrate orientation in the active site,15 (15), a feature properly referred to as "substrate-assisted catalysis".16 (16). Thus, although the hydroxylation reactions producing 17-OH PREG and 17-OH PROG are commonly accepted to be mediated by P450 compound I, the mechanism of the lyase reaction, converting 17-OH PREG to DHEA, has been intensively debated, based on results of extensive structural and functional studies.[5,9,14,17,18] One of the proposed schemes is illustrated with red arrows in Fig. 2,[4,5,8,9] where it is suggested that the conversion is initiated by attack of the nucleophilic Fe-O-O fragment of the peroxo-intermediate on the electrophilic C_{20} carbon of the substrate, generating an unstable peroxo-hemiacetal derivative that would then decay to yield DHEA and acetic acid via homolytic or heterolytic scission of the dioxygen bond.[5,9,19] Although attractive, the validity of this scheme, or other proposed schemes, awaits experimental confirmation by physical or temporal isolation and structural characterization of the key intermediates in this C-C bond cleavage reaction. A difficulty in the case of the steroidogenic cytochromes P450 is the inherently high reactivity of the encountered peroxo- and hydroperoxo-intermediates, coupled with impressively efficient delivery of protons to the active site Fe-O-O fragment. This obstacle has made temporal isolation of these fleeting species especially challenging, requiring the application of cryoradiolysis, a technique applied successfully to many systems by Symons, Hoffman, and their coworkers.[20-22] Here, this low-temperature method allows reduction of a stabilized ferrous dioxygen state while effectively restricting associated proton transfer, as we have shown for other P450 systems.[21-24]

Recognizing the need to trap adequate quantities of the initial ferric superoxide intermediate effectively, we used the previously developed nanodisc (ND) methodology, which efficiently self-assembles the full-length CYP17A1 membrane protein into a nanoscale lipid bilayer (ND/CYP17A1) to eliminate aggregation and provide full functionality, with a descriptive model shown in Fig. S1.[25] This approach has been shown to produce well-behaved assemblies of this and other membrane-bound enzymes, with the important advantage that such entities effectively enhance the stabilities of the dioxygen adducts of these enzymes,[25,26] allowing them to be efficiently prepared and quickly trapped at liquid nitrogen temperature. Indeed, our previously reported resonance Raman (rR) spectroscopy studies,[27]

Proceedings of the National Academy of Sciences, Vol 112, No. 52 (December 2015): pg. 15856-15861. DOI.

which focused on the trapped dioxygen adducts of CYP17A1 bound with its natural substrates, clearly showed that H-bonding interactions between the Fe-O-O fragments and active site residues, including bound substrates, produce telltale vibrational frequency shifts that effectively differentiate functionally significant H-bonding interactions to the proximal (p) or terminal (t) atoms within the $Fe\text{-}O_p\text{-}O_t$ fragment.[28,29] Specifically, our work on the CYP17A1 dioxygen adducts demonstrated that of the four natural substrates of CYP17A1 (Fig. 1), only 17-OH PREG was properly positioned to donate an H-bond to the proximal oxygen of the Fe-O-O fragment, an interaction that was suggested likely to persist in the subsequent peroxo-intermediate, a suggestion that is now shown to be valid by the data presented herein (*vide infra*). This finding was important, showing that the particular substrate efficiently processed in the lyase step of metabolism is also the only one that adopts an orientation that effectively intercepts the fleeting peroxo-intermediate and facilitates its attack on the juxtaposed electrophilic C_{20} atom.[30,31] Although the rR data obtained for the dioxygen intermediate of 17-OH PREG-bound CYP17A1 provided evidence suggesting the existence of a "poised" $Fe\text{-}O_p\text{-}O_t$ peroxo-fragment, confirmation of the proposed lyase pathway demands the trapping and structural characterization of this complex and the following crucial intermediate shown in the center of Fig. 2.

Proceedings of the National Academy of Sciences, Vol 112, No. 52 (December 2015): pg. 15856-15861. DOI.

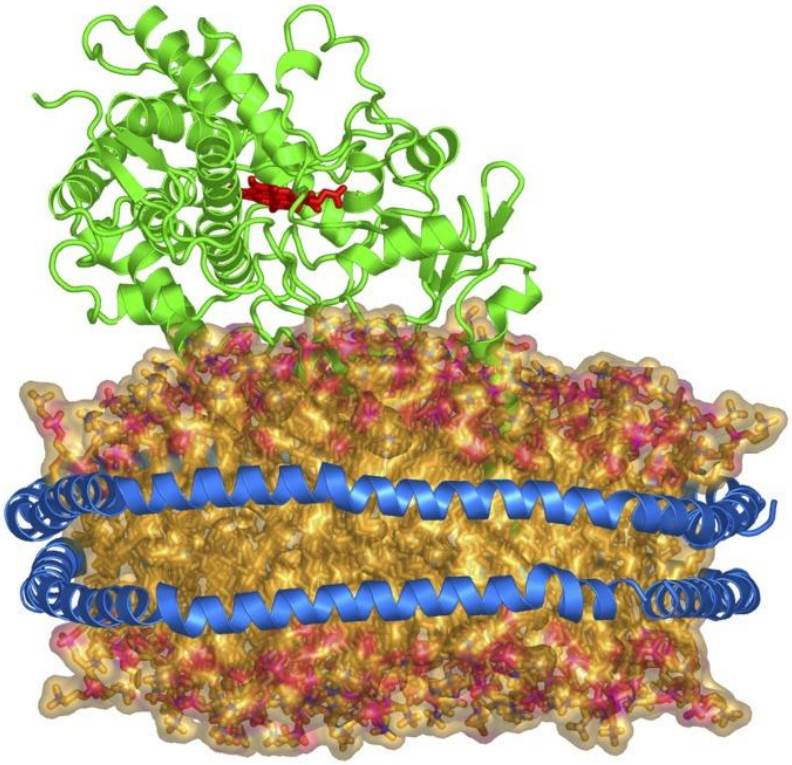

Fig. S1. Model of CYP17A1 incorporated into a nanodisc. The cytochrome P450 molecule is shown as a green cartoon representation, with heme presented in red sticks. The phospholipid bilayer is shown in orange with oxygen atoms in red, and the scaffold protein encompassing the lipid bilayer is shown as a blue cartoon representation.

Results

Detection and Temporal Evolution of Enzymatic Intermediates.

To monitor the formation and decay of the reactive intermediates encountered in the C-C bond cleavage stage of androgen biosynthesis, we first prepared the oxy-ferrous derivative of CYP17A1 in a solution of buffer containing 60% (vol/vol) glycerol along with saturating concentrations of the appropriate substrate, holding the temperature at −30 °C. Anaerobic reduction of the protein, followed by the addition of oxygen gas to the sample at low temperature, permits formation of oxy-ferrous protein with nearly 100% yield. The sample was immediately cooled to 77 K and then exposed to a 4-Mrad dose from a ^{60}Co source to generate hydrated

Proceedings of the National Academy of Sciences, Vol 112, No. 52 (December 2015): pg. 15856-15861. DOI.

electrons, which can migrate at 77 K to produce the initial peroxo-intermediate (complete details are provided in *Methods*). The relevant reaction is initiated by raising the temperature from liquid nitrogen temperatures to ~200 K while recording optical spectra.

The results are shown in Fig. 3, where samples containing either PREG (Fig. 3*A*) or 17-OH PREG (Fig. 3*B*) exhibit a strong (negative) absorption band, appearing near 440 nm in the difference spectra. This observation is consistent with the initial production and expected disappearance of the peroxo-ferric P450 species as the temperature is raised.[23,24] We note that any hydroperoxo-intermediate present in the cryoradiolytically reduced samples, generated by effective proton delivery even at 77 K, would also absorb near 440 nm.[24] Quite interesting differences are observed upon annealing either the PREG or 17-OH PREG sample to higher temperatures. The sample containing PREG, when annealed through 77–190 K, shows a steady loss of the peroxo-/hydroperoxo-intermediate (near 440 nm), converting directly to a species that exhibits an absorption spectrum that matches the absorption spectrum of the LS ferric state (λ = 417 nm) acquired at 77 K. This behavior is consistent with the rapid progression through the typical O-O bond cleavage cycle (green arrows in Fig. 2), with facile formation and rapid decay of compound I and immediate appearance of product, behavior previously observed for several bacterial P450s.[32,33] Notably, however, during an identical temperature excursion for the sample possessing 17-OH PREG, the decay of the peroxo-like Soret band at 437 nm was accompanied by the intriguing formation of a previously unidentified species with a Soret maximum near 405 nm.

Proceedings of the National Academy of Sciences, Vol 112, No. 52 (December 2015): pg. 15856-15861. DOI.

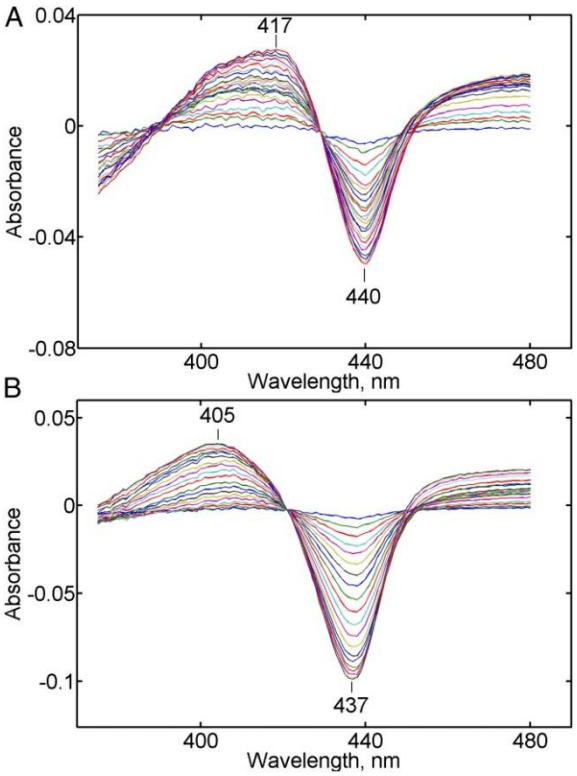

Fig. 3. Thermal annealing of peroxo-ferric intermediates monitored by optical absorption spectroscopy in CYP17A1 with different substrates PREG (A) and 17-OH PREG (B). Shown are difference spectra obtained by subtracting the spectrum at 160 K from the spectra measured at temperatures gradually increasing from 161 K (baseline) to 185 K (maximal difference).

Structural Definition of the Crucial Intermediates.

Having confirmed the existence of a 405-nm intermediate for the sample containing 17-OH PREG, we exploited the impressive power of rR spectroscopy, which is able to provide definitive structural characterization of such trapped species, revealing telltale shifts of the internal vibrational modes of the Fe-O-O fragments in response to even quite subtle, but functionally significant, active site structural changes.[23,34] The essential results of such studies are collected in Fig. 4, where the $^{16}O_2$-$^{18}O_2$ difference traces are plotted. As shown in Figs. S2–S5, the subtraction procedure cancels all heme modes (nonshifting), which clutter the raw spectra, thereby clearly revealing the isolated v(O-O) and v(Fe-O) vibrational modes of interest. Focusing first on the sample containing PREG, which is eventually processed by CYP17A1 to yield 17-OH PREG via mediation of the compound I intermediate, two sets of oxygen isotope-sensitive

Proceedings of the National Academy of Sciences, Vol 112, No. 52 (December 2015): pg. 15856-15861. DOI.

($^{16}O_2/^{18}O_2$) modes are clearly seen in the ^{16}O-^{18}O difference traces of the initial cryoreduced samples (Fig. 4*A*), signaling the presence of two intermediates. One species exhibits a $\nu(^{16}O$-$^{16}O)$ mode at 802 cm^{-1}, with its corresponding $\nu(^{18}O$-$^{18}O)$ at 764 cm^{-1} ($\Delta 16/18$ = 38 cm^{-1}), and a $\nu(Fe$-$^{16}O)$ at 554 cm^{-1}, with its $\nu(Fe$-$^{18}O)$ mode appearing at 527 cm^{-1} ($\Delta 16/18$ = 27 cm^{-1}). It is seen that these features do not shift in the difference trace generated for the samples prepared in D_2O (bottom trace in Fig. 4*A*). The lack of an observable hydrogen/deuterium (H/D) shift is entirely consistent with assignment of this set of bands to a trapped ferric peroxo-intermediate of CYP17A1. The second species in this sample exhibits a $\nu(^{16}O$-$^{16}O)$ mode at 775 cm^{-1}, which shifts to 738 cm^{-1} for the ^{18}O-analog ($\Delta 16/18$ = 37 cm^{-1}), and a corresponding $\nu(Fe$-$^{16}O)$ at 572 cm^{-1}, shifting to 545 cm^{-1} for $^{18}O_2$ ($\Delta 16/18$ = 27 cm^{-1}). It is noted that these observed ^{16}O-^{18}O isotope shifts are consistent with the isotope shifts predicted for Fe-O-O or Fe-O-O-H fragments.[35] Furthermore, the spectra of samples acquired in buffers prepared with D_2O reveal that the 775/572 cm^{-1} modes shift significantly, confirming the identification of this species as the hydroperoxo-derivative, an observation documenting the fact that a significant fraction of the peroxo-intermediate is converted to the hydroperoxo-intermediate, even at 77 K. This finding is particularly important, revealing the fact that when PREG is bound to CYP17A1, the active site architecture is intricately arranged so as to promote especially efficient proton transfer, thereby facilitating formation of compound I and the classical hydroxylation reaction required to produce 17-OH PREG.

Proceedings of the National Academy of Sciences, Vol 112, No. 52 (December 2015): pg. 15856-15861. DOI.

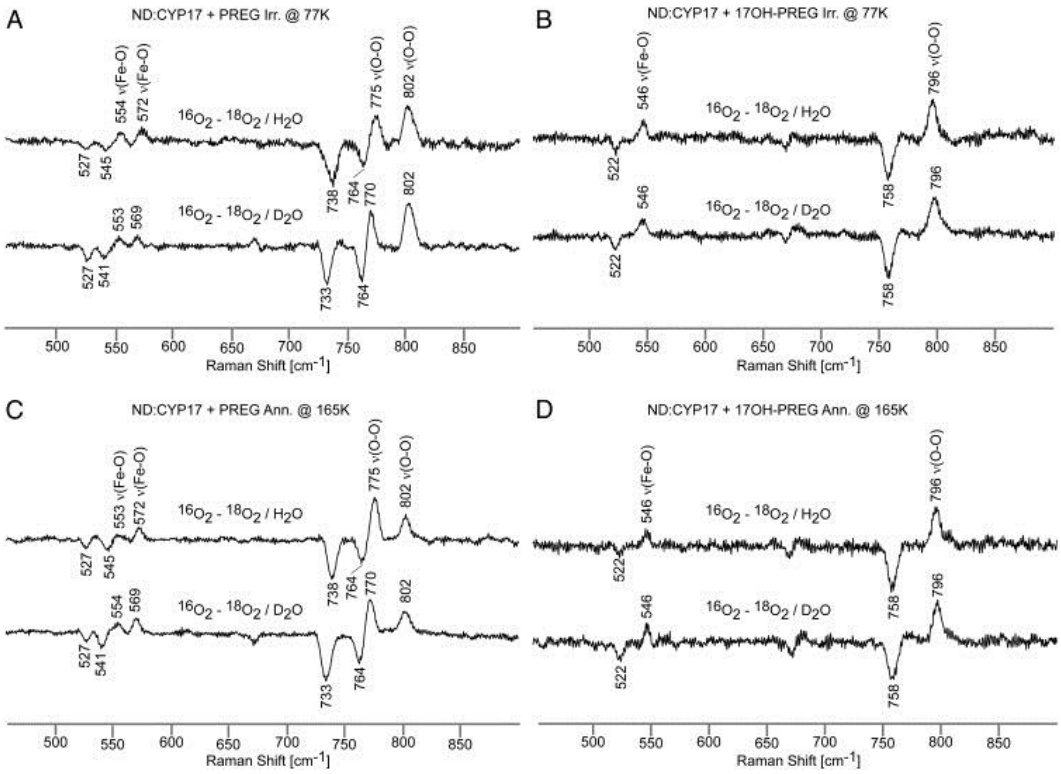

Fig. 4. rR spectral data for irradiated dioxygen adducts of CYP17A1. All spectra were measured with a 442-nm excitation line at 77 K, and the total collection time of each spectrum was 6 h. The rR $^{16}O_2$-$^{18}O_2$ difference traces in H_2O and D_2O buffers of irradiated oxy-CYP17A1 samples (before annealing) with PREG (*A*) and 17-OH PREG (*B*) and corresponding samples after annealing to 165 K (*C*) and (*D*) are shown. Using the isolated bands for the ^{16}O-peroxo (802 cm^{-1}) and ^{18}O-hydroperoxo (738 cm^{-1}) species, the I_{738}/I_{802} increases from 0.72 to 1.42. Similar values were obtained using the data from samples prepared with D_2O buffers (from 0.77 to 1.59). Ann., annealed; Irr., irradiated.

Proceedings of the National Academy of Sciences, Vol 112, No. 52 (December 2015): pg. 15856-15861. DOI.

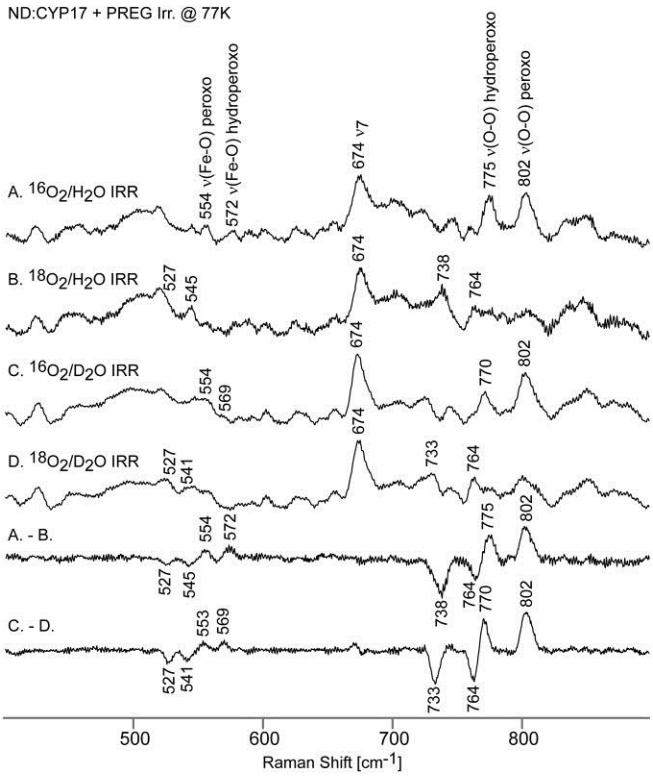

Fig. S2. Low-frequency rR spectra of irradiated (IRR) oxy-ND/CYP17A1 samples with PREG, $^{16}O_2/H_2O$ (*A*), $^{18}O_2/H_2O$ (*B*), $^{16}O_2/D_2O$ (*C*), $^{18}O_2/D_2O$ (*D*), and their difference traces are indicated. Spectra were measured with a 442-nm excitation line at 77 K, and the total collection time of each spectrum was 6 h. The modes associated with hydroperoxo-species exhibit a 5 to 3 cm^{-1} downshift in D_2O buffer. The percentages of peroxo- and hydroperoxo- species are approximately equal. The difference traces were obtained by subtracting the $^{18}O_2$ spectrum from the $^{16}O_2$ spectrum in H_2O (*Upper*) or D_2O (*Lower*) buffer. Then, the absolute spectra and difference traces were corrected using linear functions in the regions where the oxygen-sensitive modes are present.

Proceedings of the National Academy of Sciences, Vol 112, No. 52 (December 2015): pg. 15856-15861. DOI.

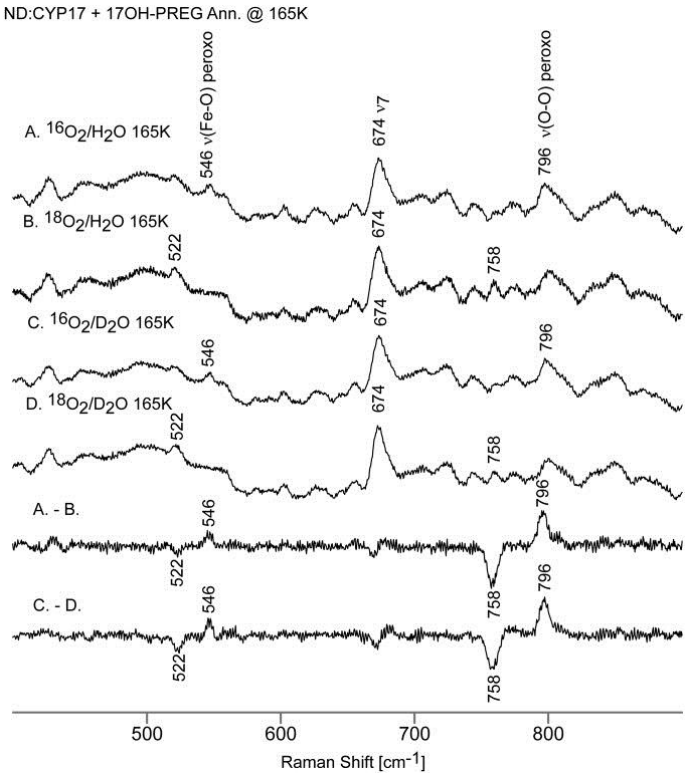

Fig. S5. Low-frequency rR spectra of irradiated and annealed at 165 K oxy-ND/CYP17A1 samples with 17OH-PREG, $^{16}O_2/H_2O$ (*A*), $^{18}O_2/H_2O$ (*B*), $^{16}O_2/D_2O$ (*C*), $^{18}O_2/D_2O$ (*D*), and their difference traces. Spectra were measured with a 442-nm excitation line at 77 K, with the total collection time of each spectrum being 6 h. No new species were detected that could be assigned to either the acylperoxo- or hydroperoxo-form. The approximate loss of intensity of modes associated with the Fe-O-O fragment is 40–50% as judged by comparison with the ν_7 mode at 674 cm^{-1}, which serves as an internal standard.

Proceedings of the National Academy of Sciences, Vol 112, No. 52 (December 2015): pg. 15856-15861. DOI.

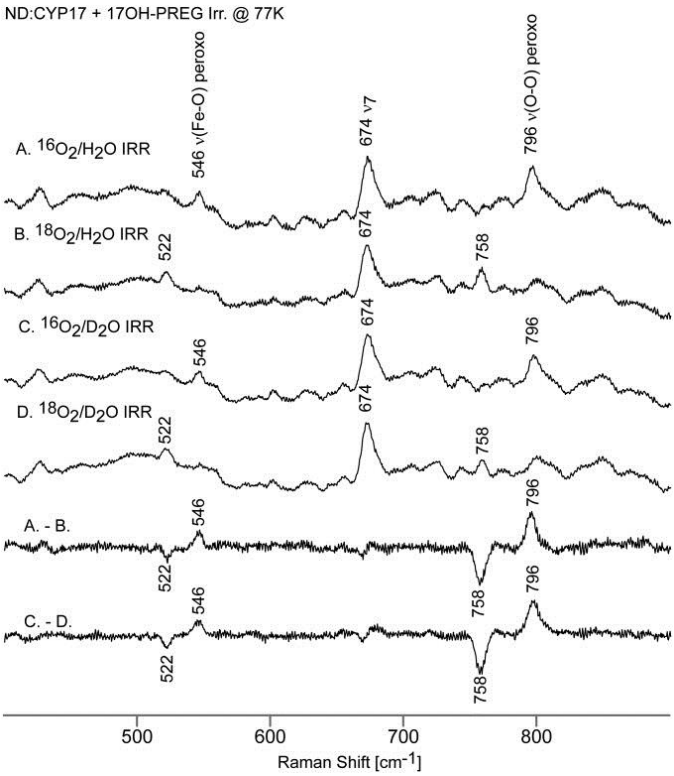

Fig. S3. Low-frequency rR spectra of irradiated oxy-ND/CYP17A1 samples with 17OH-PREG, $^{16}O_2/H_2O$ (*A*), $^{18}O_2/H_2O$ (*B*), $^{16}O_2/D_2O$ (*C*), $^{18}O_2/D_2O$ (*D*), and their difference traces are indicated. Spectra were measured with a 442-nm excitation line at 77 K, and the total collection time of each spectrum was 6 h. There is only one ν(O-O) mode and one ν(Fe-O) mode that do not have H/D sensitivity and are assigned to the peroxo-species.

Proceedings of the National Academy of Sciences, Vol 112, No. 52 (December 2015): pg. 15856-15861. DOI.

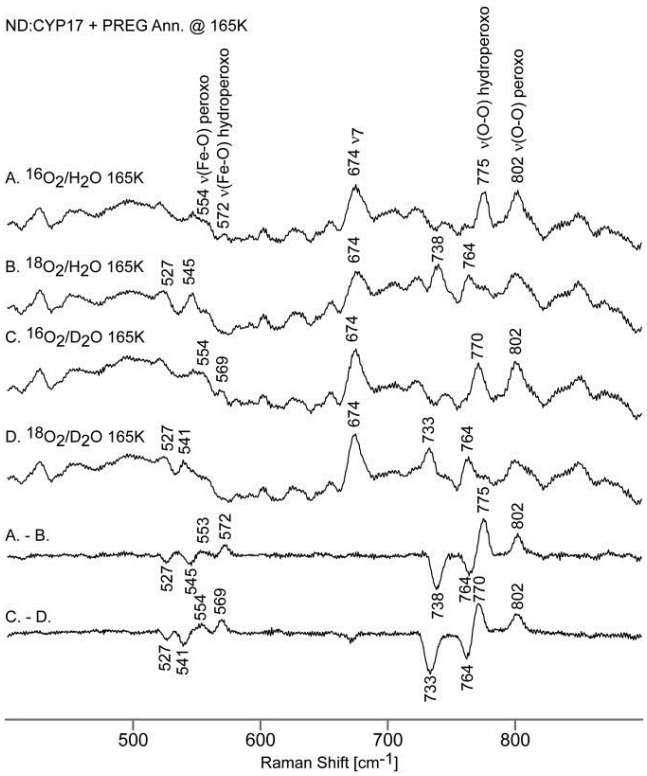

Fig. S4. Low-frequency rR spectra of irradiated and annealed (Ann.) at 165 K oxy-ND/CYP17A1 samples with PREG, $^{16}O_2/H_2O$ (*A*), $^{18}O_2/H_2O$ (*B*), $^{16}O_2/D_2O$ (*C*), $^{18}O_2/D_2O$ (*D*), and their difference traces. Spectra were measured with a 442-nm excitation line at 77 K, and the total collection time of each spectrum was 6 h. The intensity ratio of ν(O-O) of hydroperoxo-species to ν(O-O) of peroxo-species is ~2:1.

In the case of the 17-OH PREG-bound sample (Fig. 4*B*), where an additional H-bonding molecular fragment is introduced to the immediate heme environment by the substrate, the initial product of cryoradiolysis at 77 K exhibits a ν(^{16}O-^{16}O) mode at 796 cm^{-1} (Δ16/18 = 38 cm^{-1}), with the corresponding ν(Fe-^{16}O) mode occurring at 546 cm^{-1} (Δ16/18 = 24 cm^{-1}). Furthermore, it is clear from viewing the spectra obtained for the samples prepared with D_2O (bottom trace of Fig. 4*B*) that the observed modes are insensitive to the H/D exchange, with such behavior confirming the identity of this species as a ferric peroxo-intermediate, but with a slightly different disposition than the disposition seen for the PREG-bound sample. In fact, as we made clear in our earlier rR study of the dioxygen adducts of CYP17A1,[27] the lowered ν(Fe-^{16}O) frequency of the peroxo-form of the 17-OH PREG sample (546 cm^{-1}), relative to the peroxo-form of the PREG-bound sample (554 cm^{-1}), suggests that an H-bonding interaction occurs between the hydroxyl group of the substrate and the proximal oxygen

Proceedings of the National Academy of Sciences, Vol 112, No. 52 (December 2015): pg. 15856-15861. DOI.

atom of the Fe-O_p-O_t peroxo-fragment [i.e., the H-bonding seen in the dioxygen adduct persists in the peroxo-species, as we had suggested in our earlier work.[27]]. This finding is important, because such a specifically directed H-bonding interaction to the O_p of the peroxo-fragment is expected to facilitate its involvement in the lyase phase of catalysis.[30,31] This result suggests the 17-OH PREG-bound peroxo-intermediate is poised for attack upon the susceptible electrophilic C_{20} carbon of the bound substrate.

Turning our attention to efforts to trap and characterize structurally the key intermediate proposed in the center of Fig. 2, the following observations were made. The results of rR experiments using 442-nm excitation (Fig. 4*C*) show that annealing of the PREG-bound sample to 165 K causes clean conversion of the peroxo-intermediate to more of the hydroperoxo-intermediate involved in the hydroxylation pathway, with the extent of conversion being estimated to be a factor of approximately twofold, as explained in the legend of Fig. 4. Interestingly, similar annealing studies of the 17-OH PREG-bound sample provide no evidence for the appearance of any new $^{16}O/^{18}O$-sensitive bands (Fig. 4*D*). However, this outcome is not surprising, given that Fig. 3*B* shows that the newly arising second intermediate has its Soret maximum near 405 nm, far from resonance with the 442-nm excitation line. Indeed, rR spectral measurements on annealed samples, using the 406-nm excitation line from an available Krypton ion laser (Fig. 5), yielded a new set of strongly enhanced bands appearing at 791 cm^{-1} ($^{16}O_2$ sample) and 749 cm^{-1} ($^{18}O_2$ sample). The lack of an observable shift for samples prepared in D_2O-based buffer (bottom trace of Fig. 5) confirms this species does not possess a bound hydroperoxo-fragment. Furthermore, as is shown in Fig. S6, rR studies conducted with 413-nm excitation confirm that as the temperature is increased from 165 to 190 K, the intensity of this band increases relative to the intensity of "internal standard" ν(O-O) bands of the residual dioxygen adduct. This rR spectral result is entirely consistent with the increase of the 405-nm electronic absorption band over the same temperature excursion (Fig. 3*B*). It is noted that a control experiment conducted on the PREG-bound sample annealed to 190 K, using the same 406-nm excitation line (Fig. S7), did not show any evidence for a feature appearing near 790 cm^{-1}, indicating that the peroxo-hemiacetal intermediate is encountered only with the 17-OH PREG substrate, but not with the PREG substrate.

Proceedings of the National Academy of Sciences, Vol 112, No. 52 (December 2015): pg. 15856-15861. DOI.

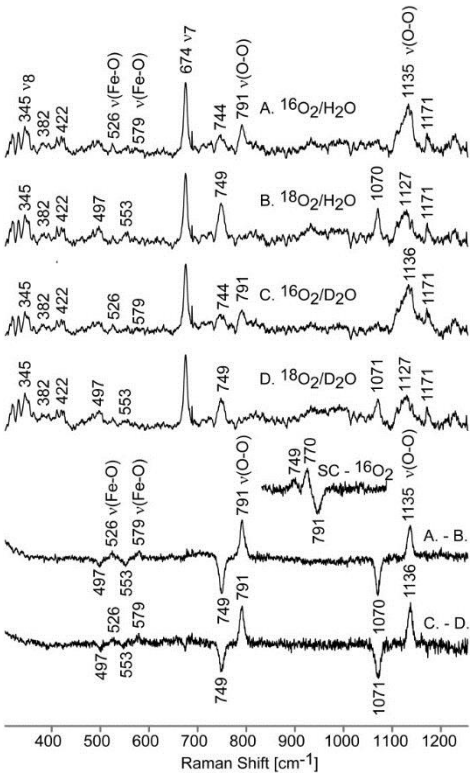

Fig. 5. rR spectral data for irradiated dioxygen adducts of CYP17A1 samples with 17-OH PREG annealed at 190 K. $^{16}O_2/H_2O$ (*A*), $^{18}O_2/H_2O$ (*B*), $^{16}O_2/D_2O$ (*C*), $^{18}O_2/D_2O$ (*D*), and their $^{16}O_2$-$^{18}O_2$ difference traces. (*D*, *Inset*) Difference trace of scrambled oxygen (SC) and the $^{16}O_2$ spectrum. Spectra were measured with a 406-nm excitation line at 77 K, and the total collection time of each spectrum was 8–9 h.

Proceedings of the National Academy of Sciences, Vol 112, No. 52 (December 2015): pg. 15856-15861. DOI.

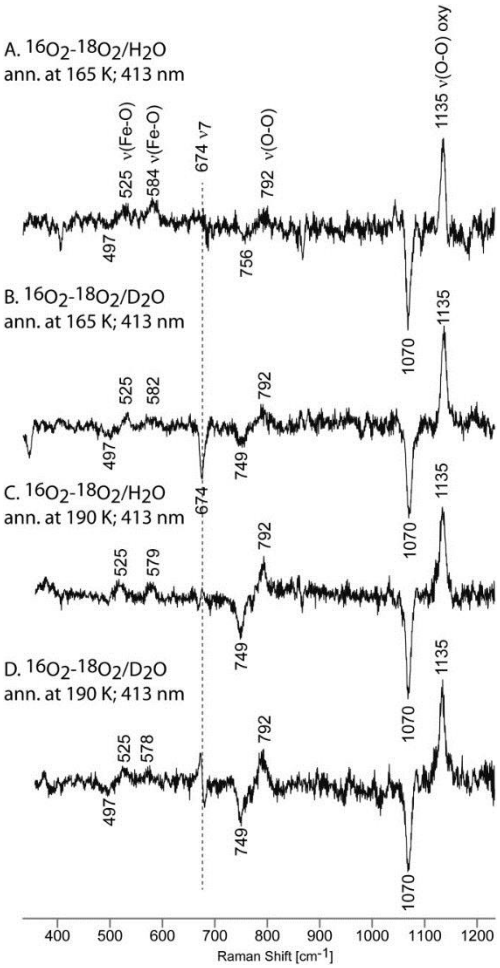

Fig. S6. $^{16}O_2$-$^{18}O_2$ difference traces of oxy-ND/CYP17A1 samples with 17OH-PREG irradiated and annealed at 165 K in H_2O buffer (*A*), in D_2O buffer (*B*), annealed at 190 K in H_2O buffer (*C*), and in D_2O buffer (*D*). Spectra were measured with a 413.1-nm excitation line at 77 K. The total collection time of each spectrum was 6–8 h. The ν(O-O) modes of residual ferrous dioxygen adducts at 1,135 cm^{-1} and 1,070 cm^{-1} were used as internal standards to evaluate the intensity increase of the new oxygen-sensitive species at around 790 cm^{-1}.

Proceedings of the National Academy of Sciences, Vol 112, No. 52 (December 2015): pg. 15856-15861. DOI.

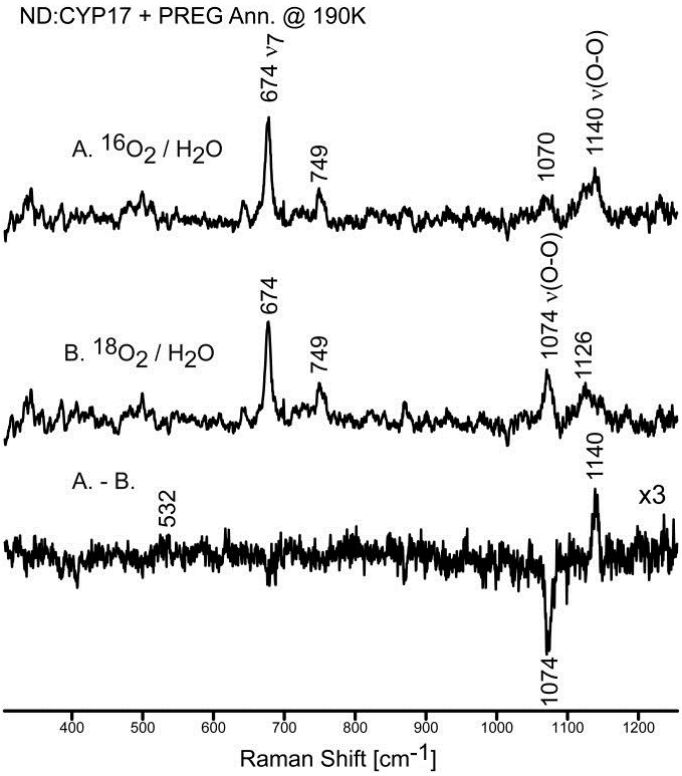

Fig. S7. rR spectra of irradiated and annealed at 190 K oxy-ND/CYP17A1 samples with PREG, $^{16}O_2/H_2O$ (*A*), $^{18}O_2/H_2O$ (*B*), and their difference traces. Spectra were measured with a 406-nm excitation line at 77 K. The total collection time of each spectrum was 4 h. The spectra show only the presence of v(O-O) modes of the residual precursor dioxygen adducts. In contrast to the case with 17OH-PREG–bound samples (Fig. 5), which displayed a 791-cm^{-1} mode of the peroxo-hemiacetal intermediate, and whose intensity was comparable to the intensity of the residual dioxygen adduct, there are no oxygen-sensitive modes observed near 790 cm^{-1} in the difference trace.

Although the observation of this single feature, appearing at 791 cm^{-1}, is obviously consistent with an intermediate with "peroxo-like" character, it must be noted that this vibrational frequency and $^{16}O/^{18}O$ isotopic shifts are close to what is expected for the v(Fe = O) mode of a ferryl heme species; the frequencies of such ferryl species depend on the transaxial ligand and distal pocket interactions, with reported values ranging from 745 cm^{-1} up to about 800 cm^{-1}.[34,36] However, the assignment of this feature to a ferryl species was ruled out by experiments conducted with scrambled oxygen, a (1:2:1) mixture of $^{16}O_2/^{16}O^{18}O/^{18}O_2$. As seen in Fig. 5 (*Inset*), and more fully documented in Fig. S8, a distinctive difference pattern emerges when subtracting the spectrum of the $^{16}O_2$ sample from the spectrum of a sample prepared with scrambled dioxygen. If the 791 cm^{-1}/749 cm^{-1} pair arises from a ferryl species (generated through O-O bond cleavage), a

Proceedings of the National Academy of Sciences, Vol 112, No. 52 (December 2015): pg. 15856-15861. DOI.

clean two-component difference pattern (Fe-^{16}O and Fe-^{18}O) would be observed in the trace shown in Fig. 5 (*Inset*). However, we clearly see a third band at 770 cm^{-1}, confirming the fact that the observed intermediate contains an intact O-O bond (i.e., ^{16}O-^{18}O), consistent with the structure proposed in the center of Fig. 2. Finally, it is also noted that the corresponding iron-oxygen ν(Fe-O) modes, expected to be seen for such a peroxo-like intermediate, are indeed seen as weak features appearing at 580 cm^{-1} ($^{16}O_2$) and 553 cm^{-1} ($^{18}O_2$). Collectively, these spectroscopic data establish the nature of the intermediate as the peroxo-hemiacetal depicted in the center of Fig. 2.

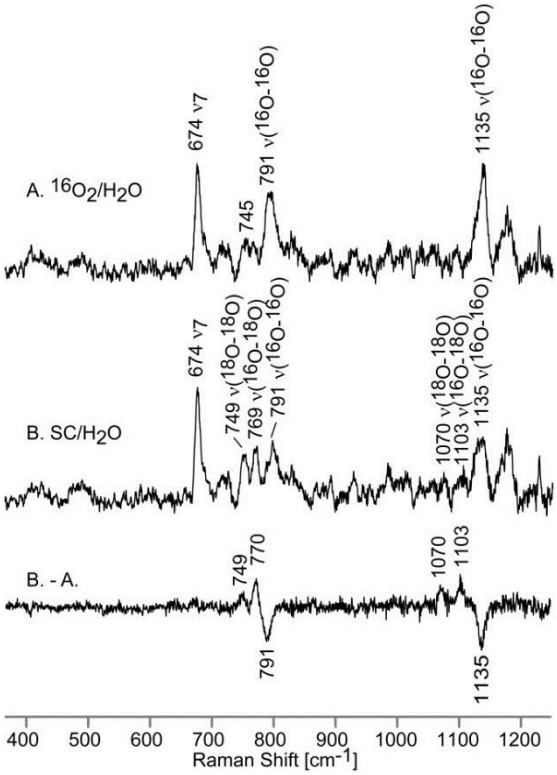

Fig. S8. rR spectra of irradiated and annealed at 190 K oxy-ND/CYP17A1 samples with 17OH-PREG, $^{16}O_2/H_2O$ (*A*), $^{16}O^{18}O$ (*B*), and their difference traces. Spectra were measured with a 406-nm excitation line at 77 K. The total collection time of each spectrum was 8 h. SC, scrambled oxygen.

Further support for this structural interpretation of the species trapped at 190 K is provided from previous studies of other iron-oxygen systems, whose structures are closely related to this intermediate (e.g., acylperoxo-adducts of heme- and nonheme proteins that possess an Fe-O-O peroxo-fragment linked to an oxidized carbon). Unlike the red-shifted Soret band at 435–440 nm

Proceedings of the National Academy of Sciences, Vol 112, No. 52 (December 2015): pg. 15856-15861. DOI.

characteristic for hydroperoxo-ferric intermediates in P450 enzymes,[23,24] a blue-shifted Soret maximum at 405 nm (Fig. 3*B*) is consistent with the bands seen for an acylperoxo-species derived from metachloroperoxybenzoic acid (mCPBA),[37,38] as well as other substituted peroxybenzoic acids.[39] In all cases, the Soret maximum varies from 413 nm for the mCPBA adduct down to 409 nm with electron-donating groups, such as the p-methoxy analog. Thus, the 405-nm maximum for the peroxo-hemiacetal intermediate, with its relatively less electrophilic carbon atom compared with the acylperoxo-species, is not unexpected. A more convincing argument for the validity of the assigned structure can be made by noting that Que and coworkers[40] have recently isolated and spectroscopically characterized an acylperoxo-derivative of a nonheme iron protein, reporting a value of 792 cm^{-1} for the frequency of the v(O-O) mode, a virtually identical value (791 cm^{-1}) to the value we observe for the assigned peroxo-hemiacetal intermediate.

The results presented here, obtained through the combined application of nanodisc methodology, cryoreduction, and rR and optical spectroscopies, reveal that owing to the highly directional H-bonding interaction between the hydroxyl group of 17-OH PREG and the proximal oxygen of the ferric peroxo-anion, this intermediate is poised for attack on the C_{20} carbon atom of the substrate. Furthermore, methodical application of the structure-sensitive rR technique, using judicious isotopic labeling strategies, provides convincing evidence that the resulting crucial intermediate of this lyase reaction is indeed the previously proposed peroxo-hemiacetal derivative. Collectively, these studies provide an elegantly simple explanation of how even quite subtle changes in active site architecture of CYP17A1, imposed by molecular fragments of the substrate, can lead to altered enzymatic pathways that carry profound physiological consequences.

Methods

Expression and Purification of CYP17A1 and Incorporation into Nanodiscs.

A gene for full-length human CYP17A1 was synthesized (DNA 2.0), including a C-terminal penta-histidine tag as well as

Proceedings of the National Academy of Sciences, Vol 112, No. 52 (December 2015): pg. 15856-15861. DOI.

modifications to the first twenty-four 5′ bases as described by Imai et al.,[41] and ligated into the pCWori$^+$ vector. DH5α was cotransformed with the resultant plasmid, as well as chaperone plasmid pGro7 containing the GroEL/ES chaperone system. Expression was then carried out using the method devised by Waterman and coworkers,[42] and purification was performed as documented previously.[27] The resultant detergent-solubilized CYP17A1 was then inserted into nanodiscs with a 1-palmitoyl-2-oleoyl-*sn*-glycero-3-phosphocholine membrane used as described by Luthra et al.[25]

Preparation of Samples for rR Spectroscopy.

The rR samples contained 280 μM ND/CYP17A1 in 100 mM potassium phosphate (pH 7.4), 250 mM sodium chloride, 30% (vol/vol) distilled glycerol, 6.24 μM methyl viologen, and either 450 μM PREG or 400 μM OH-PREG. Deuterated samples were prepared by exhaustive exchange into identical buffer adjusted to pD 7.4 [electrode calibrated by method of Glasoe and Long[43]] prepared with 100% D_2O and distilled glycerol-d_3. Ferric samples were then contained in 5-mm-OD NMR tubes (WG-5 ECONOMY; Wilmad) and de-aerated under argon for 5 min, followed by reduction under anaerobic conditions with a 1.5-fold molar excess of sodium dithionite. Each sample was then transferred to a dry ice-ethanol bath held at −15 °C, where it was cooled for 1 min. Oxy-ferrous complexes were formed by addition of $^{16}O_2$, $^{18}O_2$, or $^{16}O^{18}O$ scrambled oxygen) for 10 s, followed by rapid freezing in liquid N_2. Frozen samples containing oxy-ferrous CYP17A1 were subsequently radiolytically reduced to the peroxo-state by a 4-Mrad dose of gamma-rays in a Gammacell 200 Excel ^{60}Co source while immersed in liquid nitrogen as described previously.[44]

rR Measurements.

Samples of irradiated oxy-ND/CYP17A1 were excited using a 441.6-nm line provided by a He-Cd laser (IK Series He-Cd laser; Kimmon Koha Co.), whereas the samples annealed to 190 K were measured with 406.7- and 413.1-nm excitation lines from a Kr^+ laser (Coherent Innova Sabre Ion Laser). The rR spectra of all samples were measured using a Spex 1269 spectrometer equipped with Spec-10 LN-cooled detector (Princeton Instruments). The slit width was set at 150

Proceedings of the National Academy of Sciences, Vol 112, No. 52 (December 2015): pg. 15856-15861. DOI.

μm, and the 1,200-g/mm grating was used; with this grating, the resultant spectral dispersion is 0.46 cm^{-1} per pixel. The laser power was kept at ~1 mW or less to minimize photodissociation. Moreover, to avoid laser-induced heating and protein degradation, the samples were contained in spinning NMR tubes (5-mm outside diameter, WG-5 ECONOMY; Wilmad). The 180° backscattering geometry was used for all measurements, and the laser beam was focused onto the sample using a cylindrical lens.[45] The NMR tubes were positioned into a double-walled quartz low-temperature cell filled with liquid nitrogen. All measurements were done at 77 K, and total collection time was around 6 h for the irradiated samples and ~8–9 h for the annealed samples. Spectra were calibrated with fenchone (Sigma–Aldrich) and processed with GRAMS/32 AI software (Galactic Industries).

Preparation of Optical Samples and Collection of Optical Spectra.

Methods of preparation and collection of optical samples containing P450 in the peroxo-state have been described in detail previously.[24,44] Briefly, ND/CYP17A1 in 100 mM potassium phosphate (pH 7.4), 15% (vol/vol) glycerol, and 400 μM PREG or 17-OH PREG were anaerobically reduced with a 1.5-fold molar excess of sodium dithionite with the aid of methyl viologen at a 1:40 ratio of redox mediator to P450. Oxy-ferrous CYP17A1 was formed by rapid injection of this solution into 100 mM potassium phosphate (pH 7.4) buffer containing 67.5% (vol/vol) glycerol contained in a methacrylate cuvette and chilled to 243 K. After 25 s of vigorous mixing, the sample was rapidly cooled to 210 K, and then to 77 K at a rate of ~4 $K \cdot min^{-1}$. The final concentration of ND/CYP17A1 and glycerol was ~30 μM and 60% (vol/vol), respectively. Samples were irradiated as described previously (*Methods*, *Preparation of Samples for rR Spectroscopy*), and then photobleached for 30 min under a 100-W tungsten-halogen lamp behind a 450-nm long-pass filter while immersed in liquid nitrogen. Spectra were collected in a home-built optical cryostat[46] aligned within the beam path of a Cary 300 spectrophotometer as the temperature was increased linearly at a rate of ~1 $K \cdot min^{-1}$.

Proceedings of the National Academy of Sciences, Vol 112, No. 52 (December 2015): pg. 15856-15861. DOI.

Acknowledgments

We appreciate the help provided by Dr. Jay A. LaVerne, Notre Dame Radiation Laboratory (Notre Dame University), a facility of the US Department of Energy, Office of Basic Energy Science. This work was supported by grants from the NIH, including Grants GM96117 (to J.R.K.), GM33775 (to S.G.S.), and GM110428 (to S.G.S. and J.R.K.).

Footnotes

The authors declare no conflict of interest.
This article is a PNAS Direct Submission.
This article contains supporting information online at www.pnas.org/lookup/suppl/doi:10.1073/pnas.1519376113/-/DCSupplemental.

References

1. Huggins C, Hodges CV. Studies on prostatic cancer: I. The effect of castration, of estrogen and of androgen injection on serum phosphatases in metastatic carcinoma of the prostate. 1941. *J Urol.* 2002;168(1):9–12.
2. Gomez L, Kovac JR, Lamb DJ. CYP17A1 inhibitors in castration-resistant prostate cancer. *Steroids*. 2015;95:80–87.
3. Porubek D. CYP17A1: A biochemistry, chemistry, and clinical review. *Curr Top Med Chem*. 2013;13(12):1364–1384.
4. Ortiz de Montellano PR, editor. *Cytochrome P450 Structure, Mechanism and Biochemistry*. 3rd Ed Kluwer/Plenum; New York: 2005.
5. Hrycay EG, Bandiera SM, editors. *Advances in Experimental Medicine and Biology*. Vol 851 Springer; London: 2015. Monooxygenase, Peroxidase and Peroxygenase Properties and Mechanisms of Cytochrome P450.
6. Nakajin S, Hall PF. Microsomal cytochrome P-450 from neonatal pig testis. Purification and properties of A C_{21} steroid side-chain cleavage system (17 α-hydroxylase-$C_{17,20}$ lyase) *J Biol Chem*. 1981;256(8):3871–3876.
7. Nakajin S, Shively JE, Yuan PM, Hall PF. Microsomal cytochrome P-450 from neonatal pig testis: Two enzymatic activities (17 α-hydroxylase and $c_{17,20}$-lyase) associated with one protein. *Biochemistry*. 1981;20(14):4037–4042.
8. Gilep AA, Sushko TA, Usanov SA. At the crossroads of steroid hormone biosynthesis: The role, substrate specificity and evolutionary development of CYP17. *Biochim Biophys Acta*. 2011;1814(1):200–209.

9. Akhtar M, Wright JN, Lee-Robichaud P. A review of mechanistic studies on aromatase (CYP19) and 17α-hydroxylase-17,20-lyase (CYP17) *J Steroid Biochem Mol Biol*. 2011;125(1-2):2–12.
10. Mathieu AP, LeHoux JG, Auchus RJ. Molecular dynamics of substrate complexes with hamster cytochrome P450c17 (CYP17): Mechanistic approach to understanding substrate binding and activities. *Biochim Biophys Acta*. 2003;1619(3):291–300.
11. Auchus RJ. The genetics, pathophysiology, and management of human deficiencies of P450c17. *Endocrinol Metab Clin North Am*. 2001;30(1):101–119, vii.
12. Rittle J, Green MT. Cytochrome P450 compound I: Capture, characterization, and C-H bond activation kinetics. Science. 2010;330(6006):933–937.
13. Yosca TH, et al. Iron(IV)hydroxide pK(a) and the role of thiolate ligation in C-H bond activation by cytochrome P450. *Science*. 2013;342(6160):825–829.
14. Pallan PS, et al. Structural and kinetic basis of steroid 17α,20-lyase activity in teleost fish cytochrome P450 17A1 and its absence in cytochrome P450 17A2. *J Biol Chem*. 2015;290(6):3248–3268. [
15. DeVore NM, Scott EE. Structures of cytochrome P450 17A1 with prostate cancer drugs abiraterone and TOK-001. *Nature*. 2012;482(7383):116–119.
16. Cupp-Vickery JR, Han O, Hutchinson CR, Poulos TL. Substrate-assisted catalysis in cytochrome P450eryF. *Nat Struct Biol*. 1996;3(7):632–637.
17. Akhtar M, Corina D, Miller S, Shyadehi AZ, Wright JN. Mechanism of the acyl-carbon cleavage and related reactions catalyzed by multifunctional P-450s: Studies on cytochrome P-450(17)alpha. *Biochemistry*. 1994;33(14):4410–4418.
18. Gregory MC, Denisov IG, Grinkova YV, Khatri Y, Sligar SG. Kinetic solvent isotope effect in human P450 CYP17A1-mediated androgen formation: evidence for a reactive peroxoanion intermediate. *J Am Chem Soc.* 2013;135(44):16245–16247.
19. Akhtar M, Corina DL, Miller SL, Shyadehi AZ, Wright JN. Incorporation of label from $^{18}O_2$ into acetate during side-chain cleavage catalysed by cytochrome P-45017α(17α-hydroxylase-17,20-lyase) *J Chem Soc Perkin* 1. 1994;(3):263–267.
20. Kappl R, Hoehn-Berlage M, Huettermann J, Bartlett N, Symons MCR. Electron spin and electron nuclear double resonance of the [FeO_2]-[ferrite] center from irradiated oxyhemo- and oxymyoglobin. *Biochim Biophys Acta*. 1985;827(3):327–343.

Proceedings of the National Academy of Sciences, Vol 112, No. 52 (December 2015): pg. 15856-15861. DOI.

21. Davydov R, Hoffman BM. Active intermediates in heme monooxygenase reactions as revealed by cryoreduction/annealing, EPR/ENDOR studies. *Arch Biochem Biophys*. 2011;507(1):36–43.
22. Denisov IG, Grinkova YV, Sligar SG. Cryoradiolysis and cryospectroscopy for studies of heme-oxygen intermediates in cytochromes p450. *Methods Mol Biol*. 2012;875:375–391.
23. Denisov IG, Mak PJ, Makris TM, Sligar SG, Kincaid JR. Resonance Raman characterization of the peroxo and hydroperoxo intermediates in cytochrome P450. *J Phys Chem A*. 2008;112(50):13172–13179.
24. Denisov IG, Makris TM, Sligar SG. Cryotrapped reaction intermediates of cytochrome p450 studied by radiolytic reduction with phosphorus-32. *J Biol Chem*. 2001;276(15):11648–11652.
25. Luthra A, Gregory M, Grinkova YV, Denisov IG, Sligar SG. Nanodiscs in the studies of membrane-bound cytochrome P450 enzymes. *Methods Mol Biol*. 2013;987:115–127.
26. Grinkova YV, et al. The ferrous-oxy complex of human aromatase. *Biochem Biophys Res Commun*. 2008;372(2):379–382.
27. Gregory M, Mak PJ, Sligar SG, Kincaid JR. Differential hydrogen bonding in human CYP17 dictates hydroxylation versus lyase chemistry. *Angew Chem Int Ed Engl*. 2013;52(20):5342–5345.
28. Spiro TG, Soldatova AV. Ambidentate H-bonding of NO and O_2 in heme proteins. *J Inorg Biochem*. 2012;115:204–210.
29. Spiro TG, Soldatova AV, Balakrishnan G. CO, NO and O_2 as vibrational probes of heme protein interactions. *Coord Chem Rev*. 2013;257(2):511–527.
30. Harris DL, Loew GH. Theoretical investigation of the proton assisted pathway to formation of cytochrome P450 Compound I. *J Am Chem Soc.* 1998;120(35):8941–8948.
31. Ogliaro F, de Visser SP, Cohen S, Sharma PK, Shaik S. Searching for the second oxidant in the catalytic cycle of cytochrome P450: A theoretical investigation of the iron(III)-hydroperoxo species and its epoxidation pathways. *J Am Chem Soc*. 2002;124(11):2806–2817.
32. Davydov R, et al. Hydroxylation of camphor by reduced oxy-cytochrome P450cam: Mechanistic implications of EPR and ENDOR studies of catalytic intermediates in native and mutant enzymes. *J Am Chem Soc.* 2001;123(7):1403–1415.
33. Davydov R, Macdonald IDG, Makris TM, Sligar SG, Hoffman BM. EPR and ENDOR of catalytic intermediates in cryoreduced native and mutant oxy-cytochromes P450cam: Mutation-induced changes in the proton delivery system. *J Am Chem Soc*. 1999;121(45):10654–10655.
34. Mak PJ, Thammawichai W, Wiedenhoeft D, Kincaid JR. Resonance Raman spectroscopy reveals pH-dependent active site structural changes of

lactoperoxidase compound 0 and its ferryl heme O-O bond cleavage products. *J Am Chem Soc*. 2015;137(1):349–361.
35. Nakamoto K. Infrared and Raman Spectra of Inorganic and Coordination Compounds, *Part A: Theory and Applications in Inorganic Chemistry*. 6th Ed Wiley; Hoboken, NJ: 2009.
36. Terner J, et al. Resonance Raman spectroscopy of oxoiron(IV) porphyrin π-cation radical and oxoiron(IV) hemes in peroxidase intermediates. *J Inorg Biochem*. 2006;100(4):480–501.
37. Spolitak T, Dawson JH, Ballou DP. Reaction of ferric cytochrome P450cam with peracids: Kinetic characterization of intermediates on the reaction pathway. *J Biol Chem*. 2005;280(21):20300–20309.
38. Spolitak T, Funhoff EG, Ballou DP. Spectroscopic studies of the oxidation of ferric CYP153A6 by peracids: Insights into P450 higher oxidation states. *Arch Biochem Biophys*. 2010;493(2):184–191.
39. Collins DP. 2012. *Spectroscopic characterization of reaction intermediates of the heme-thiolate proteins*. PhD thesis (University of South Carolina, Columbia, SC)
40. Oloo WN, et al. Identification of a low-spin acylperoxoiron(III) intermediate in bio-inspired non-heme iron-catalyzed oxidations. *Nat Commun.* 2014;5:4046/1–4046/9.
41. Imai T, Globerman H, Gertner JM, Kagawa N, Waterman MR. Expression and purification of functional human 17 α-hydroxylase/17,20-lyase (P450c17) in *Escherichia coli.* Use of this system for study of a novel form of combined 17 α-hydroxylase/17,20-lyase deficiency. *J Biol Chem*. 1993;268(26):19681–19689.
42. Barnes HJ, Arlotto MP, Waterman MR. Expression and enzymatic activity of recombinant cytochrome P450 17 α-hydroxylase in Escherichia coli. *Proc Natl Acad Sci USA*. 1991;88(13):5597–5601.
43. Glasoe PK, Long FA. Use of glass electrodes to measure acidities in deuterium oxide. *J Phys Chem*. 1960;64(1):188–190.
44. Denisov IG, Makris TM, Sligar SG. Cryoradiolysis for the study of P450 reaction intermediates. *Methods Enzymol*. 2002;357:103–115.
45. Shriver DF, Dunn JBR. Backscattering geometry for Raman-spectroscopy of colored materials. *Appl Spectrosc*. 1974;28(4):319–323.
46. Luthra A, Denisov IG, Sligar SG. Temperature derivative spectroscopy to monitor the autoxidation decay of cytochromes P450. *Anal Chem*. 2011;83(13):5394–5399.

Proceedings of the National Academy of Sciences, Vol 112, No. 52 (December 2015): pg. 15856-15861. DOI.

Supporting Information

Mak et al. 10.1073/pnas.1519376113

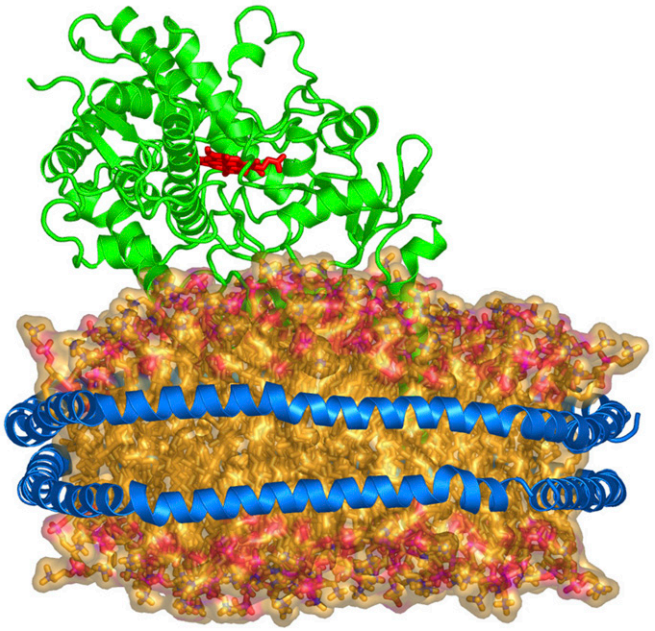

Fig. S1. Model of CYP17A1 incorporated into a nanodisc. The cytochrome P450 molecule is shown as a green cartoon representation, with heme presented in red sticks. The phospholipid bilayer is shown in orange with oxygen atoms in red, and the scaffold protein encompassing the lipid bilayer is shown as a blue cartoon representation.

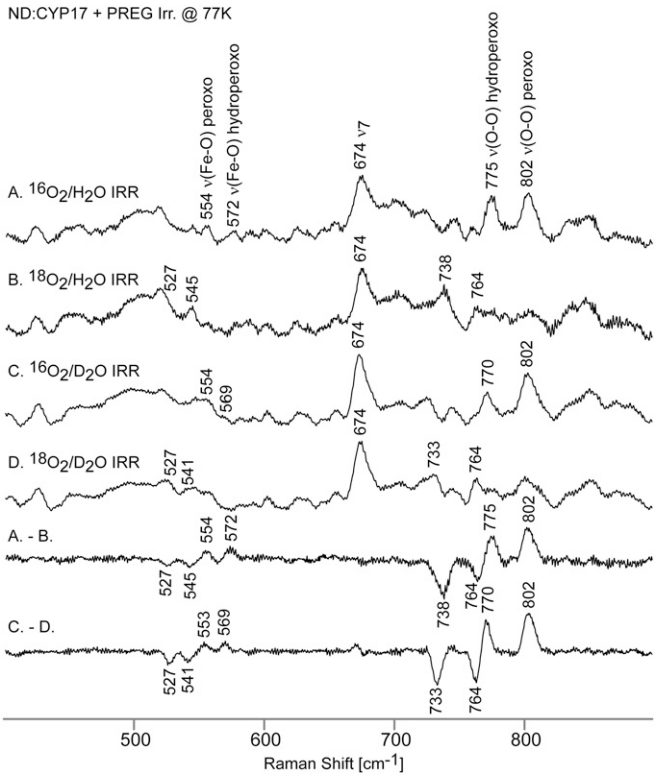

Fig. S2. Low-frequency rR spectra of irradiated (IRR) oxy-ND/CYP17A1 samples with PREG, $^{16}O_2/H_2O$ (*A*), $^{18}O_2/H_2O$ (*B*), $^{16}O_2/D_2O$ (*C*), $^{18}O_2/D_2O$ (*D*), and their difference traces are indicated. Spectra were measured with a 442-nm excitation line at 77 K, and the total collection time of each spectrum was 6 h. The modes associated with hydroperoxo-species exhibit a 5 to 3 cm^{-1} downshift in D_2O buffer. The percentages of peroxo- and hydroperoxo- species are approximately equal. The difference traces were obtained by subtracting the $^{18}O_2$ spectrum from the $^{16}O_2$ spectrum in H_2O (*Upper*) or D_2O (*Lower*) buffer. Then, the absolute spectra and difference traces were corrected using linear functions in the regions where the oxygen-sensitive modes are present.

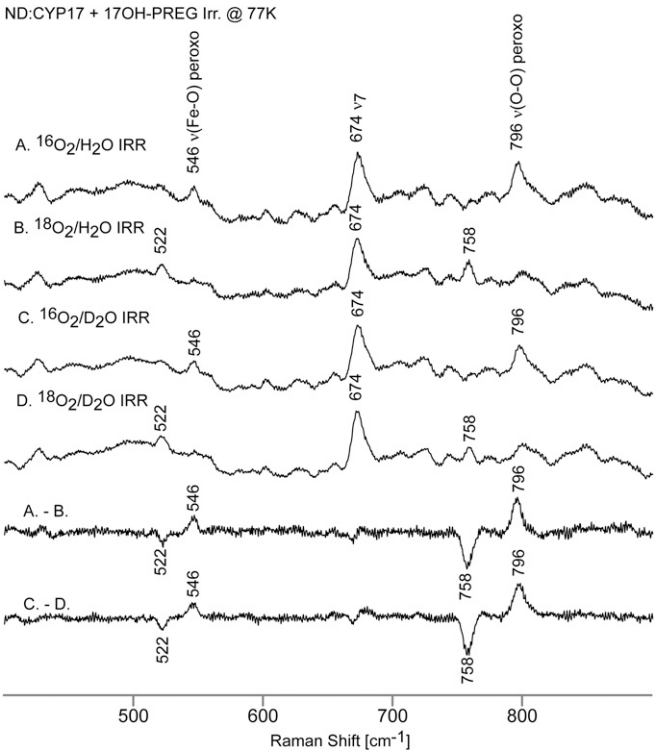

Fig. S3. Low-frequency rR spectra of irradiated oxy-ND/CYP17A1 samples with 17OH-PREG, $^{16}O_2/H_2O$ (*A*), $^{18}O_2/H_2O$ (*B*), $^{16}O_2/D_2O$ (*C*), $^{18}O_2/D_2O$ (*D*), and their difference traces are indicated. Spectra were measured with a 442-nm excitation line at 77 K, and the total collection time of each spectrum was 6 h. There is only one ν(O-O) mode and one ν(Fe-O) mode that do not have H/D sensitivity and are assigned to the peroxo-species.

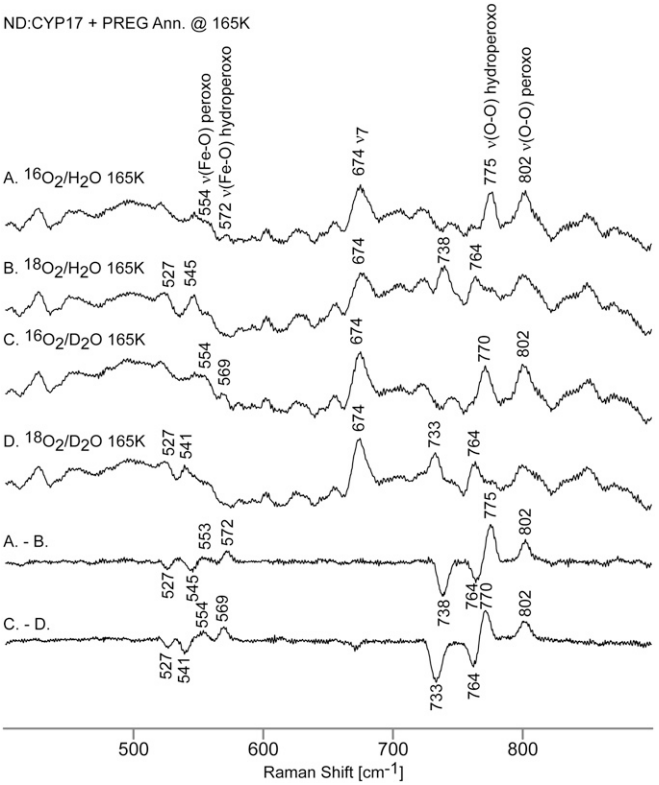

Fig. S4. Low-frequency rR spectra of irradiated and annealed (Ann.) at 165 K oxy-ND/CYP17A1 samples with PREG, $^{16}O_2/H_2O$ (*A*), $^{18}O_2/H_2O$ (*B*), $^{16}O_2/D_2O$ (*C*), $^{18}O_2/D_2O$ (*D*), and their difference traces. Spectra were measured with a 442-nm excitation line at 77 K, and the total collection time of each spectrum was 6 h. The intensity ratio of ν(O-O) of hydroperoxo-species to ν(O-O) of peroxo-species is ~2:1.

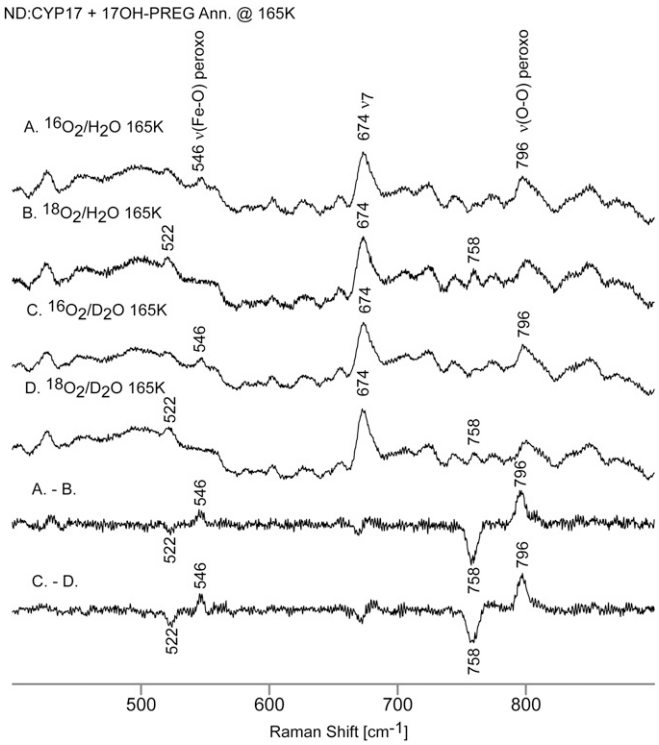

Fig. S5. Low-frequency rR spectra of irradiated and annealed at 165 K oxy-ND/CYP17A1 samples with 17OH-PREG, $^{16}O_2/H_2O$ (*A*), $^{18}O_2/H_2O$ (*B*), $^{16}O_2/D_2O$ (*C*), $^{18}O_2/D_2O$ (*D*), and their difference traces. Spectra were measured with a 442-nm excitation line at 77 K, with the total collection time of each spectrum being 6 h. No new species were detected that could be assigned to either the acylperoxo- or hydroperoxo-form. The approximate loss of intensity of modes associated with the Fe-O-O fragment is 40–50% as judged by comparison with the ν_7 mode at 674 cm^{-1}, which serves as an internal standard.

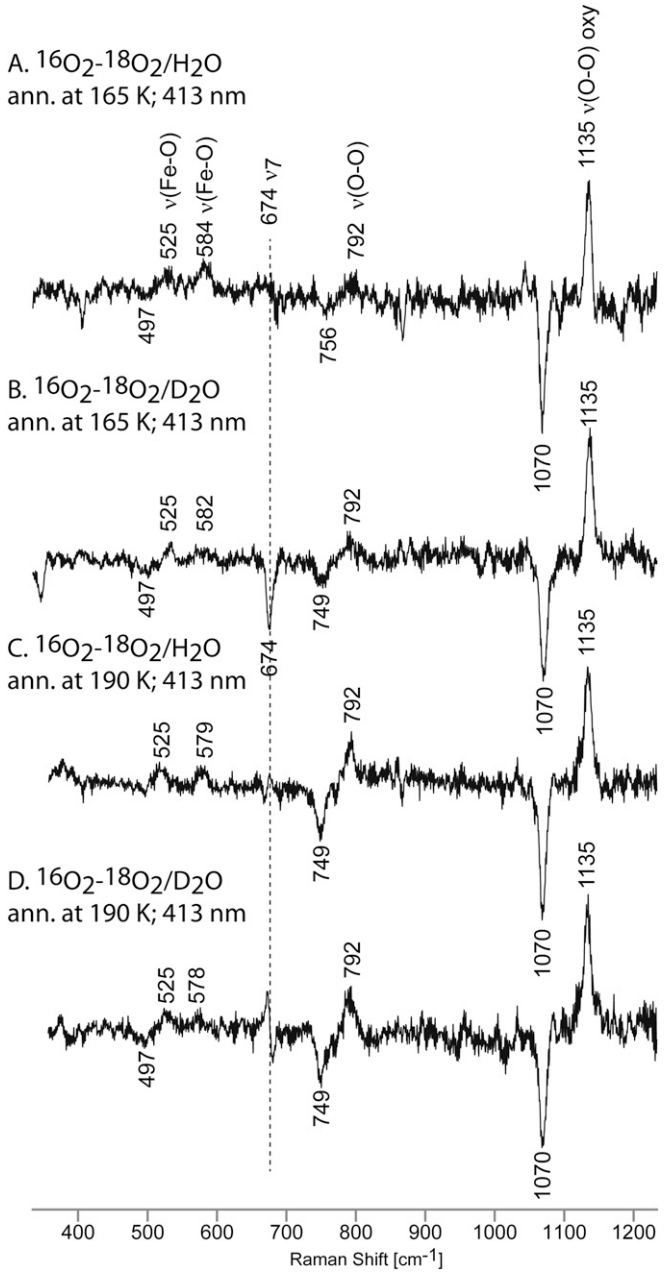

Fig. S6. $^{16}O_2$-$^{18}O_2$ difference traces of oxy-ND/CYP17A1 samples with 17OH-PREG irradiated and annealed at 165 K in H_2O buffer (*A*), in D_2O buffer (*B*), annealed at 190 K in H_2O buffer (*C*), and in D_2O buffer (*D*). Spectra were measured with a 413.1-nm excitation line at 77 K. The total collection time of each spectrum was 6–8 h. The ν(O-O) modes of residual ferrous dioxygen adducts at 1,135 cm^{-1} and 1,070 cm^{-1} were used as internal standards to evaluate the intensity increase of the new oxygen-sensitive species at around 790 cm^{-1}.

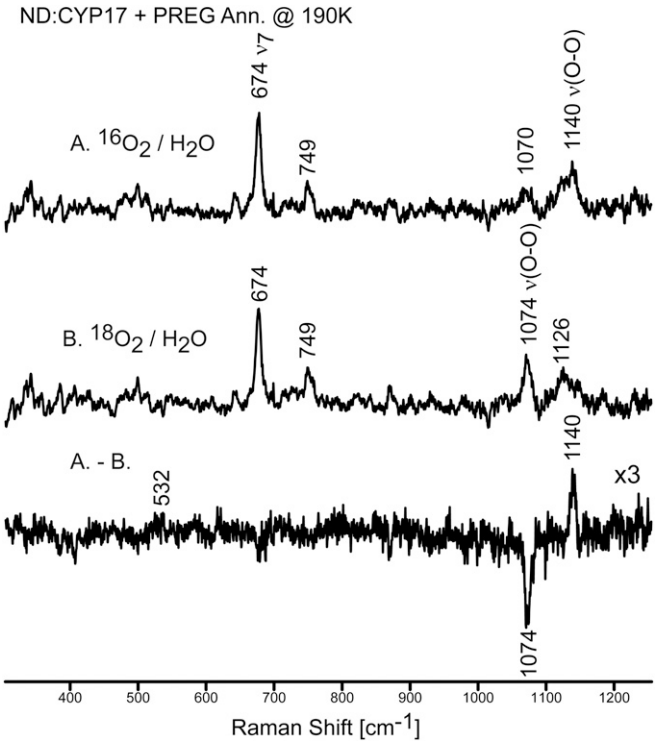

Fig. S7. rR spectra of irradiated and annealed at 190 K oxy-ND/CYP17A1 samples with PREG, $^{16}O_2/H_2O$ (*A*), $^{18}O_2/H_2O$ (*B*), and their difference traces. Spectra were measured with a 406-nm excitation line at 77 K. The total collection time of each spectrum was 4 h. The spectra show only the presence of ν(O-O) modes of the residual precursor dioxygen adducts. In contrast to the case with 17OH-PREG–bound samples (Fig. 5), which displayed a 791-cm^{-1} mode of the peroxo-hemiacetal intermediate, and whose intensity was comparable to the intensity of the residual dioxygen adduct, there are no oxygen-sensitive modes observed near 790 cm^{-1} in the difference trace.

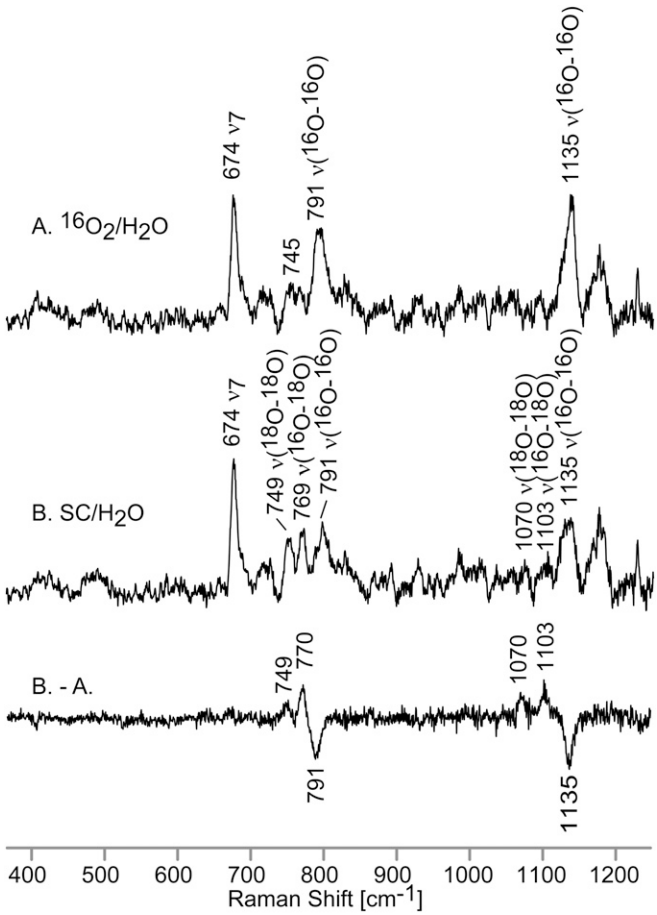

Fig. S8. rR spectra of irradiated and annealed at 190 K oxy-ND/CYP17A1 samples with 17OH-PREG, $^{16}O_2/H_2O$ (*A*), $^{16}O^{18}O$ (*B*), and their difference traces. Spectra were measured with a 406-nm excitation line at 77 K. The total collection time of each spectrum was 8 h. SC, scrambled oxygen.